PERGAMON

International Journal of Solids and Structures 40 (2003) 4299–4318

INTERNATIONAL JOURNAL OF SOLIDS and STRUCTURES

www.elsevier.com/locate/ijsolstr

A thermodynamically consistent large deformation elastic–viscoplastic model with directional tensile failure

M.B. Rubin [a,*], I. Lomov [b]

[a] Faculty of Mechanical Engineering Technion, Israel Institute of Technology, Technion City, 32000 Haifa, Israel
[b] Geophysics and Global Security Division, Lawrence Livermore National Laboratory, Livermore, CA 94550, USA

Received 23 April 2003

Abstract

The main objective of this paper is to develop a continuum model for directional tensile failure that can simulate weakening and void formation due to tensile failure. Directionality in the model allows simulation of weakening to tension applied in one direction, without weakening to subsequent tension applied in perpendicular directions. The model is developed within the context of a properly invariant non-linear thermomechanical theory. Specifically, it is shown how the model can be combined with general constitutive equations for porous compaction and dilation, as well as viscoplasticity. The thermoelastic response is hyperelastic, with the stress being determined by derivatives of the Helmholtz free energy, and the material is considered to be elastically isotropic. In particular, it is assumed that the rate of inelasticity due to tensile failure is coaxial with the tensor measure of elastic deformation (and hence stress). This causes the rate of dissipation to take a particularly simple form which can be shown to satisfy the second law of thermodynamics. A numerical procedure for integrating these evolution equations is proposed and a number of examples are considered to explore the response of the model to different loading histories.

Keywords: Directional; Porosity; Tensile failure; Thermomechanical; Viscoplastic

1. Introduction

Constitutive models for tensile failure and damage typically include one or more of the following phenomena:

(P1) a reduced yield strength;
(P2) a reduced elastic modulus; and
(P3) an evolving void strain.

These models can remain isotropic or they can introduce anisotropic damage.

* Corresponding author. Tel.: +972-4-8293188; fax: +972-4-8295711.
E-mail address: mbrubin@tx.technion.ac.il (M.B. Rubin).

0020-7683/03/$ - see front matter
doi:10.1016/S0020-7683(03)00242-7

Continuum damage mechanics (e.g. Curran et al., 1987; Krajcinovic, 1996) generalizes the early work of Kachanov (1958) for rupture under creep conditions. The simplest continuum damage model includes the phenomena (P1) by introducing an evolution equation for a scalar measure of damage that reduces the magnitude of the yield strength. Another example is the Gurson model for void growth (Gurson, 1977) which introduces the effects of porosity and pressure on the yield surface in ductile metals.

More complicated models include the phenomena (P2) and introduce evolution equations for scalar and tensorial measures of damage can be used to modify the elastic stiffness of the material (e.g. Carol et al., 2001). However, when the elastic response is modified by multiple scalars or tensors, the notion of damage as a weakening of the material is not so clear (Elata and Rubin, 1994). Also, it is necessary to ensure that the second law of thermodynamics is satisfied, with the damage process being dissipative.

Using linear elastic fracture mechanics to characterize effective properties of materials containing multiple interacting idealized cracks has also been a very active research area, and an overview of this field can be found in (Nemat-Nasser and Hori, 1993; Kachanov et al., 1994). This approach is successful for linear elastic problems but generalizations for finite deformation are not straight-forward, especially when it is necessary to model the full non-linear thermomechanical coupling that is active in shock waves. Usually, attempts are made to introduce non-linear phenomenological evolution equations with coefficients and functions that incorporate features of the results of fracture mechanics (e.g. Rajendran et al., 1989). If the cracks are randomly oriented and the crack density is high then the elastic response remains reasonably isotropic. Within this framework, it is possible to develop constitutive equations for the shock response of brittle materials (e.g. Bar-on et al., 2003) which include the phenomena (P2) and (P3) by introducing a void strain through an evolution equation for porosity.

A comprehensive model for porous elastic–viscoplastic material with tensile failure that is applicable to shock problems is recorded in (Rubin et al., 2000). In this model and evolution equation for porosity is used to introduce voids and limit the amount tensile pressure. Also, the Lode angle is used to modify the yield strength to exhibit the typical characteristic of a brittle material that it fails at a much lower stress in tension than it does in compression. Moreover, since the Lode angle is an isotropic invariant of Cauchy stress these constitutive equations only model isotropic damage.

Menzel and Steinmann (2001) have recently developed a model for anisotropic continuum damage mechanics at large strains. This formulation introduces a strain energy function that depends on invariants of total strain relative to a structural tensor. Moreover, this structural tensor represents damage and is determined by an evolution equation of the type considered by Betten (1985). In their general forms, these constitutive equations are capable of modeling the phenomena (P2) and (P3).

The main objective of a constitutive model for directional tensile failure, like the one developed in this paper, is to model the fact that although a brittle material (like rock) can fail in one direction it may retain virgin strength to tensile failure in a perpendicular direction. From the mathematical point of view it is always possible to propose evolution equations for the internal state variables that ensure maximum dissipation. However, such constitutive assumption may be difficult to interpret physically. Therefore, a major challenge in the development of a theory of directional tensile failure is to develop a theoretical structure that is amenable to the analysis of physically based constitutive assumptions and is amenable to the development of a robust integration scheme.

The model developed in this paper focuses mainly on the phenomena (P3). Porosity is used as an isotropic measure of volumetric void strain and its evolution is influenced by tensile failure [see (39b)]. Furthermore, instead of introducing a void strain tensor, the inelastic effects of directional void opening and closing are modeled by introducing their effects on the rate of evolution of elastic deformation [see (36a)]. Specifically, it is assumed that the rate of inelasticity due to tensile failure is coaxial with the tensor measure of elastic deformation (and hence stress). This causes the rate of dissipation to take a particularly simple form [see (31)] which can be analyzed easily.

An outline of this paper is as follows. Section 2 briefly reviews the basic equations of continuum thermodynamics, Section 3 introduces the general constitutive structure and Section 4 proposes specific constitutive equations. Section 5 presents details of the numerical integration scheme, Section 6 discusses a number of example problems which demonstrate the predictions of the model, and Section 7 presents conclusions.

Throughout the paper bold faced symbols are used to denote tensors and $\mathbf{I}$ denotes the second order unit tensor. Also, $\mathbf{a}\cdot\mathbf{b}$ denotes the usual scalar product of two vectors $\mathbf{a}$, $\mathbf{b}$ and $\mathbf{A}\cdot\mathbf{B}=\mathrm{tr}(\mathbf{A}\mathbf{B}^{\mathrm{T}})$ denotes the scalar product of two second order tensors $\mathbf{A}$, $\mathbf{B}$. Moreover, $\mathbf{B}^{\mathrm{T}}$ denotes the transpose of $\mathbf{B}$, $\mathrm{tr}\,\mathbf{A}=\mathbf{A}\cdot\mathbf{I}$ denotes the trace operation, $\det(\mathbf{A})$ denotes the determinant of the tensor $\mathbf{A}$, and the symbol $\otimes$ denotes the tensor product operator.

2. Basic equations

By way of background it is recalled that $\mathbf{X}$ denotes the location of a material point in a fixed reference configuration, $\mathbf{x}$ denotes the location of the same material point in the deformed present configuration at time t, $\mathbf{v}=\dot{\mathbf{x}}$ denotes the absolute velocity of the material point, and $\mathbf{L}=\partial\mathbf{v}/\partial\mathbf{x}$ denotes the velocity gradient. Here, and throughout the text a superposed dot is used to denote material time differentiation holding $\mathbf{X}$ fixed.

The constitutive equations are developed using the thermodynamical procedures proposed by Green and Naghdi (1977, 1978). Within this context, the usual laws of conservation of mass and balances of linear momentum, angular momentum and energy are supplemented by a balance of entropy which in local form is written as

$$\rho\dot{\eta}=\rho(s+\xi)-\mathrm{div}\,\mathbf{p}, \tag{1}$$

where ρ is the mass per unit present volume, η is the specific (per unit mass) entropy, s is the specific external rate of supply of entropy, ξ is the specific rate of internal production of entropy, $\mathbf{p}$ is the entropy flux per unit present surface area, and div denotes the divergence operator in the present position $\mathbf{x}$. Also, it is recalled that s and $\mathbf{p}$ are related to the absolute temperature θ, the specific external rate of heat supply r, and the heat flux vector $\mathbf{q}$ that appear in the energy equation by the expressions

$$s=\frac{r}{\theta},\qquad \mathbf{p}=\frac{\mathbf{q}}{\theta}. \tag{2}$$

In general, ξ can be separated into two parts

$$\rho\theta\xi=-\mathbf{p}\cdot\mathbf{g}+\rho\theta\xi', \tag{3}$$

where $\mathbf{g}=\partial\theta/\partial\mathbf{x}$ is the temperature gradient with respect to the present position. One part $(-\mathbf{p}\cdot\mathbf{g})$ is related to the entropy production due to heat conduction and another part $(\rho\theta\xi')$ is related to the entropy production due to material dissipation (Rubin, 1986).

Using (1)–(3) the rate of heat supplied to the body can be written in the form

$$\rho r-\mathrm{div}\,\mathbf{q}=\rho\theta\dot{\eta}-\rho\theta\xi'. \tag{4}$$

Thus, the local form of the balance of energy can be expressed in the equivalent forms

$$\rho\dot{\varepsilon}=\rho r-\mathrm{div}\,\mathbf{q}+\mathbf{T}\cdot\mathbf{D},\qquad \rho\theta\xi'=\mathbf{T}\cdot\mathbf{D}-\rho(\dot{\psi}+\eta\dot{\theta}), \tag{5a, b}$$

where the specific Helmholtz free energy ψ and the specific internal energy ε are related by the expression

$$\psi=\varepsilon-\theta\eta. \tag{6}$$

Also, $\mathbf{T}$ is the Cauchy stress tensor and $\mathbf{D}$ is the symmetric part of the velocity gradient $\mathbf{L}$.

Constitutive assumptions for the quantities

$$\{\psi, \eta, \varepsilon, \mathbf{T}, \mathbf{p}, \xi'\}, \tag{7}$$

are restricted by the usual invariance conditions under superposed rigid body motions and by the requirements that the balance of angular momentum

$$\mathbf{T}^{\mathrm{T}} = \mathbf{T}, \tag{8}$$

and the balance of energy (5b) be satisfied for all thermomechanical processes. Furthermore, these constitutive equations are required to satisfy statements of the second law of thermodynamics with include the condition that heat flows from hot to cold

$$-\mathbf{p} \cdot \mathbf{g} > 0 \quad \text{for } \mathbf{g} \neq 0, \tag{9}$$

and the condition that the material dissipation is non-negative

$$\rho\theta\xi' \geqslant 0. \tag{10}$$

3. Constitutive equations

In contrast with standard approaches to plasticity which introduce measures of inelastic deformation through evolution equations, the approach taken here is motivated by the works of Eckart (1948) and Leonov (1976) who propose evolution equations directly for elastic deformation measures. Additional physical reasons for abandoning measures of plastic deformation can be found in (Rubin, 1994, 1996, 2001). Specifically, within the context of the proposed model it is convenient to introduce a measure of elastic deformation as a symmetric, invertible, positive definite tensor $\mathbf{B}_{\mathrm{e}}$ which is determined by integrating the evolution equation

$$\dot{\mathbf{B}}_{\mathrm{e}} = \mathbf{L}\mathbf{B}_{\mathrm{e}} + \mathbf{B}_{\mathrm{e}}\mathbf{L}^{\mathrm{T}} - J_{\mathrm{e}}^{2/3}\mathbf{A}, \tag{11}$$

where J_{e} is a pure measure of elastic dilatation

$$J_{\mathrm{e}}^2 = \det(\mathbf{B}_{\mathrm{e}}). \tag{12}$$

The tensor $\mathbf{A}$ includes the inelastic effects of the rate of plastic deformation as well as that due to directional tensile failure. Moreover, with the help of the work of Flory (1961), it is possible to define $\mathbf{B}'_{\mathrm{e}}$ as a unimodular tensor which is a pure measure of elastic distortional deformation

$$\mathbf{B}'_{\mathrm{e}} = J_{\mathrm{e}}^{-2/3}\mathbf{B}_{\mathrm{e}}, \qquad \det(\mathbf{B}'_{\mathrm{e}}) = 1. \tag{13}$$

Also, using the fact that

$$\frac{\mathrm{d}[\det(\mathbf{B}_{\mathrm{e}})]}{\mathrm{d}t} = \det(\mathbf{B}_{\mathrm{e}})\mathbf{B}_{\mathrm{e}}^{-1} \cdot \dot{\mathbf{B}}_{\mathrm{e}}, \tag{14}$$

it can be shown that J_{e} and $\mathbf{B}'_{\mathrm{e}}$ are determined by the evolution equations

$$\frac{\dot{J}_{\mathrm{e}}}{J_{\mathrm{e}}} = \mathbf{D} \cdot \mathbf{I} - \frac{1}{2}\mathbf{A} \cdot \mathbf{B}_{\mathrm{e}}^{\prime -1}, \tag{15a}$$

$$\dot{\mathbf{B}}'_{\mathrm{e}} = \mathbf{L}\mathbf{B}'_{\mathrm{e}} + \mathbf{B}'_{\mathrm{e}}\mathbf{L}^{\mathrm{T}} - \tfrac{2}{3}(\mathbf{D} \cdot \mathbf{I})\mathbf{B}'_{\mathrm{e}} - \left[\mathbf{A} - \tfrac{1}{3}(\mathbf{A} \cdot \mathbf{B}_{\mathrm{e}}^{\prime -1})\mathbf{B}'_{\mathrm{e}}\right]. \tag{15b}$$

Here, the Helmholtz free energy ψ is assumed to be a function of the variables

$$\{J_e, \mathbf{B}'_e, \theta\}. \tag{16}$$

However, since ψ must remain unaltered under superposed rigid body motions (SRBM) it follows that it can be a function of $\mathbf{B}'_e$ only through its two independent invariants

$$\alpha_1 = \mathbf{B}'_e \cdot \mathbf{I}, \qquad \alpha_2 = \mathbf{B}'_e \cdot \mathbf{B}'_e. \tag{17}$$

For simplicity, ψ is taken to be independent of α_2 so that it takes the form

$$\psi = \psi(J_e, \alpha_1, \theta). \tag{18}$$

Using this expression, the reduced form of the balance of energy (5b) yields the equation

$$\rho\theta\xi' = \left[\mathbf{T} - \rho J_e \frac{\partial\psi}{\partial J_e}\mathbf{I} - 2\rho\frac{\partial\psi}{\partial\alpha_1}\mathbf{B}''_e\right] \cdot \mathbf{D} - \rho\left[\eta + \frac{\partial\psi}{\partial\theta}\right]\dot{\theta} + \frac{1}{2}\rho J_e \frac{\partial\psi}{\partial J_e}\left[\mathbf{A} \cdot \mathbf{B}'^{-1}_e\right] + \rho\frac{\partial\psi}{\partial\alpha_1}\left[\mathbf{A} - \frac{1}{3}\left(\mathbf{A} \cdot \mathbf{B}'^{-1}_e\right)\mathbf{B}'_e\right] \cdot \mathbf{I}, \tag{19}$$

where $\mathbf{B}''_e$ is the deviatoric part of $\mathbf{B}'_e$

$$\mathbf{B}''_e = \mathbf{B}'_e - \tfrac{1}{3}(\mathbf{B}'_e \cdot \mathbf{I})\mathbf{I}. \tag{20}$$

Sufficient conditions for (19) to be satisfied for all thermomechanical processes allow the stress and the entropy to be given in the hyperelastic forms

$$\mathbf{T} = -p\mathbf{I} + \mathbf{T}', \qquad p = -\rho J_e \frac{\partial\psi}{\partial J_e}, \qquad \mathbf{T}' = 2\rho\frac{\partial\psi}{\partial\alpha_1}\mathbf{B}''_e, \qquad \eta = -\frac{\partial\psi}{\partial\theta}, \tag{21a–d}$$

where p is the pressure and $\mathbf{T}'$ is the deviatoric part of the stress. Since these forms cause the deviatoric stress $\mathbf{T}'$ to vanish when $\mathbf{B}'_e = \mathbf{I}$, the value of $\mathbf{B}'_e$ is known in any stress-free state. Moreover, the rate of dissipation becomes

$$\rho\theta\xi' = \frac{1}{2}\rho J_e \frac{\partial\psi}{\partial J_e}\left[\mathbf{A} \cdot \mathbf{B}'^{-1}_e\right] + \rho\frac{\partial\psi}{\partial\alpha_1}\left[\mathbf{A} - \frac{1}{3}\left(\mathbf{A} \cdot \mathbf{B}'^{-1}_e\right)\mathbf{B}'_e\right] \cdot \mathbf{I}. \tag{22}$$

For porous materials it is common to introduce the current value ϕ of porosity, its reference value Φ, and the reference density ρ_{s0} of the solid matrix, such that

$$J_e = \left[\frac{1-\phi}{1-\Phi}\right]J, \qquad \rho_0 = (1-\Phi)\rho_{s0}, \qquad \rho = (1-\phi)J_e^{-1}\rho_{s0}, \tag{23a–c}$$

$$\dot{J}_e = J_e\left[\mathbf{D} \cdot \mathbf{I} - \frac{\dot{\phi}}{1-\phi}\right], \tag{23d}$$

where use has been made of the conservation of mass and the rate of change of the total dilatation J

$$\rho J = \rho_0, \qquad \dot{J} = J\mathbf{D} \cdot \mathbf{I}. \tag{24a, b}$$

Then, the constitutive equations (21) for stress can be rewritten in the more common forms (Carroll and Holt, 1972)

$$p = (1-\phi)p_s, \qquad \mathbf{T}' = (1-\phi)\mathbf{T}'_s, \tag{25a, b}$$

$$p_s = -\rho_{s0}\frac{\partial\psi}{\partial J_e}, \qquad \mathbf{T}'_s = 2J_e^{-1}\rho_{s0}\frac{\partial\psi}{\partial\alpha_1}\mathbf{B}''_e, \tag{25c, d}$$

where p_s and $\mathbf{T}'_s$ are the pressure and deviatoric stress of the solid matrix, respectively.

Next, the inelastic deformation tensor $\mathbf{A}$ is separated into a part $\mathbf{A}_p$ (Rubin and Attia, 1996) associated with viscoplasticity and a part $\mathbf{A}_v$ associated with void formation (due to porosity and cracks) due to tensile failure

$$\mathbf{A} = \mathbf{A}_p + \mathbf{A}_v, \qquad \mathbf{A}_p = \Gamma_p \left[\mathbf{B}'_e - \left\{ \frac{3}{\mathbf{B}'^{-1}_e \cdot \mathbf{I}} \right\} \mathbf{I} \right], \tag{26}$$

where the scalar Γ_p requires a constitutive equation. Thus, the rate of dissipation (22) can be written in the alternative form

$$\xi' = \xi'_d + \xi'_v, \qquad \rho\theta\xi'_d = \rho \frac{\partial \psi}{\partial \alpha_1} \Gamma_p \left[\mathbf{B}'_e \cdot \mathbf{I} - \left\{ \frac{9}{\mathbf{B}'^{-1}_e \cdot \mathbf{I}} \right\} \right], \tag{27a, b}$$

$$\rho\theta\xi'_v = \frac{1}{2}\rho J_e \frac{\partial \psi}{\partial J_e} \left[\mathbf{A}_v \cdot \mathbf{B}'^{-1}_e \right] + \rho \frac{\partial \psi}{\partial \alpha_1} \left[\mathbf{A}_v - \frac{1}{3} \left(\mathbf{A}_v \cdot \mathbf{B}'^{-1}_e \right) \mathbf{B}'_e \right] \cdot \mathbf{I}, \tag{27c}$$

where ξ'_d is related to the dissipation of plastic distortional deformation and ξ'_v is related to the dissipation of void formation.

In order to propose a constitutive equation for $\mathbf{A}_v$ it is convenient to define $\mathbf{p}_i$ as the orthonormal right-handed set of eigenvectors of $\mathbf{B}'_e$, which are ordered so that

$$\mathbf{B}'_e = \beta_1(\mathbf{p}_1 \otimes \mathbf{p}_1) + \beta_2(\mathbf{p}_2 \otimes \mathbf{p}_2) + \beta_3(\mathbf{p}_3 \otimes \mathbf{p}_3), \quad \beta_1 \geqslant \beta_2 \geqslant \beta_3 = \frac{1}{\beta_1 \beta_2} > 0. \tag{28}$$

Thus, in view of the constitutive equations (21), the stress $\mathbf{T}$ can be written in its spectral form

$$\mathbf{T} = \sigma_1(\mathbf{p}_1 \otimes \mathbf{p}_1) + \sigma_2(\mathbf{p}_2 \otimes \mathbf{p}_2) + \sigma_3(\mathbf{p}_3 \otimes \mathbf{p}_3), \quad \sigma_1 \geqslant \sigma_2 \geqslant \sigma_3, \qquad \sigma_i = -p + \sigma'_i,$$
$$\sigma'_i = 2\rho \frac{\partial \psi}{\partial \alpha_1} \left[\beta_i - \frac{1}{3}(\mathbf{B}'_e \cdot \mathbf{I}) \right], \tag{29}$$

where σ_i are the ordered principal stresses. Next, it is assumed that the rate of void formation tends to reduce these principal stresses so that $\mathbf{A}_v$ is specified in the form

$$\mathbf{A}_v = 2[\Gamma_{v1}\beta_1(\mathbf{p}_1 \otimes \mathbf{p}_1) + \Gamma_{v2}\beta_2(\mathbf{p}_2 \otimes \mathbf{p}_2) + \Gamma_{v3}\beta_3(\mathbf{p}_3 \otimes \mathbf{p}_3)], \tag{30}$$

where the scalar functions Γ_{vi} require constitutive equations. Thus, with the help of (21), (28)–(30), the rate of dissipation (27c) reduces to

$$\rho\theta\xi'_v = \sigma_1\Gamma_{v1} + \sigma_2\Gamma_{v2} + \sigma_3\Gamma_{v3}. \tag{31}$$

Moreover, comparison of (15a) with (23d) and use of (26) and (30) indicates that the rate of change of porosity is given in the simple form

$$\frac{\dot{\phi}}{1 - \phi} = \frac{1}{2}\mathbf{A} \cdot \mathbf{B}'^{-1}_e = \Gamma_{v1} + \Gamma_{v2} + \Gamma_{v3}. \tag{32}$$

Next, using the spectral representation (28) it can be shown that

$$\mathbf{B}'_e \cdot \mathbf{I} - \left\{ \frac{9}{\mathbf{B}'^{-1}_e \cdot \mathbf{I}} \right\} \geqslant 0. \tag{33}$$

Moreover, for the model under consideration, both $\partial\psi/\partial\alpha_1$ and Γ_p are each non-negative so plastic deformation is dissipative

$$\rho\theta\xi'_{\mathrm{d}} \geqslant 0 \quad \text{for } \left\{ \frac{\partial\psi}{\partial\alpha_1} \geqslant 0 \text{ and } \Gamma_{\mathrm{p}} \geqslant 0 \right\}. \tag{34}$$

For later convenience, the auxiliary variables Γ_{f} and $\Gamma'_{\mathrm{f}i}$ are defined so that $\Gamma_{\mathrm{v}i}$ can be written in the forms

$$\Gamma_{\mathrm{v}i} = \frac{\Gamma_{\mathrm{I}}}{3} + \Gamma_{\mathrm{f}i}, \qquad \Gamma_{\mathrm{f}} = \Gamma_{\mathrm{f1}} + \Gamma_{\mathrm{f2}} + \Gamma_{\mathrm{f3}}, \qquad \Gamma'_{\mathrm{f}i} = \Gamma_{\mathrm{f}i} - \frac{\Gamma_{\mathrm{f}}}{3}. \tag{35}$$

Then, with the help of (26), (28) and (30), the dissipation (31), the rate of change of porosity (32), and the rate of elastic distortional deformation (15b) can be rewritten in the forms

$$\xi'_{\mathrm{v}} = \xi'_{\mathrm{I}} + \xi'_{\mathrm{f}}, \qquad \rho\theta\xi'_{\mathrm{I}} = -p\Gamma_{\mathrm{I}}, \qquad \rho\theta\xi'_{\mathrm{f}} = \sigma_1\Gamma_{\mathrm{f1}} + \sigma_2\Gamma_{\mathrm{f2}} + \sigma_3\Gamma_{\mathrm{f3}}, \tag{36a–c}$$

$$\frac{\dot{\phi}}{1-\phi} = \Gamma_{\mathrm{I}} + \Gamma_{\mathrm{f}}, \tag{36d}$$

$$\dot{\mathbf{B}}'_{\mathrm{e}} = \mathbf{L}\mathbf{B}'_{\mathrm{e}} + \mathbf{B}'_{\mathrm{e}}\mathbf{L}^{\mathrm{T}} - \tfrac{2}{3}(\mathbf{D}\cdot\mathbf{I})\mathbf{B}'_{\mathrm{e}} - \mathbf{A}_{\mathrm{p}} - 2\beta_1\Gamma'_{\mathrm{f1}}(\mathbf{p}_1\otimes\mathbf{p}_1) - 2\beta_2\Gamma'_{\mathrm{f2}}(\mathbf{p}_2\otimes\mathbf{p}_2) - 2\beta_3\Gamma'_{\mathrm{f3}}(\mathbf{p}_3\otimes\mathbf{p}_3). \tag{36e}$$

Here, Γ_{I} is used to characterize dilation and compaction of the isotropic component of porosity [notice that Γ_{I} does not influence the evolution of $\mathbf{B}'_{\mathrm{e}}$], and $\Gamma_{\mathrm{f}i}$ characterize void formation and collapse due to directional tensile failure. More specifically, constitutive equations will be specified so that the response to directional tensile failure is dissipative

$$\sigma_1\Gamma_{\mathrm{f1}} \geqslant 0, \qquad \sigma_2\Gamma_{\mathrm{f2}} \geqslant 0, \qquad \sigma_3\Gamma_{\mathrm{f3}} \geqslant 0, \qquad \rho\theta\xi'_{\mathrm{f}} \geqslant 0. \tag{37a–d}$$

From (36b) it can be seen that the isotropic response during compaction ($\Gamma_{\mathrm{I}} < 0$) at positive pressure, or during dilation ($\Gamma_{\mathrm{I}} > 0$) at negative pressure, each are dissipative. However, the response of "bulking" (dilation at positive pressure) is non-dissipative. In this regard it is recalled that the second law of thermodynamics (10) requires only that the total rate of dissipation be non-negative, not the individual components. Physically, bulking can occur only when distortional deformation causes changes in the topology of fragments of material. Therefore, the constitutive equation for Γ_{I} should be limited so that the non-dissipative effects of bulking never dominate the dissipative effects of plastic deformation

$$\rho\theta\xi'_{\mathrm{d}} + \rho\theta\xi'_{\mathrm{I}} \geqslant 0. \tag{38}$$

Furthermore, for later convenience, the isotropic porosity ϕ_{I}, and directional failure porosity ϕ_{f} are defined so that

$$\frac{\dot{\phi}_{\mathrm{I}}}{1-\phi} = \Gamma_{\mathrm{I}}, \qquad \frac{\dot{\phi}_{\mathrm{f}}}{1-\phi} = \Gamma_{\mathrm{f}}, \qquad \phi = \phi_{\mathrm{I}} + \phi_{\mathrm{f}}. \tag{39a–c}$$

In calculating the elastic distortional deformation using the evolution equation (36e) there is no need to introduce a tensorial measure of plastic strain. Instead, the inelasticity due to plastic deformation is introduced through the rate $\mathbf{A}_{\mathrm{p}}$. If desired, it is possible to introduce the equivalent plastic strain ε_{p} through the evolution equation

$$\dot{\varepsilon}_{\mathrm{p}} = \left[\tfrac{2}{3}\mathbf{D}_{\mathrm{p}}\cdot\mathbf{D}_{\mathrm{p}}\right]^{1/2}, \qquad \mathbf{D}_{\mathrm{p}} = \tfrac{1}{2}\mathbf{A}_{\mathrm{p}}. \tag{40a, b}$$

Next, it is convenient to introduce a symmetric tensor $\boldsymbol{\Delta}$, which is interpreted as the distribution of damage due to directional tensile failure. In particular, the damage Δ in a general direction $\mathbf{n}$ ($\mathbf{n}\cdot\mathbf{n} = 1$) and the damage Δ_i in the principal directions of stress $\mathbf{p}_i$ are defined by

$$\Delta = \langle \boldsymbol{\Delta}\cdot(\mathbf{n}\otimes\mathbf{n})\rangle, \qquad \Delta_i = \langle \boldsymbol{\Delta}\cdot(\mathbf{p}_i\otimes\mathbf{p}_i)\rangle \quad (\text{no sum on } i), \tag{41}$$

where $\langle x\rangle$ represent the Macauley brackets

$$\langle x\rangle = \tfrac{1}{2}[x+|x|]. \tag{42}$$

Thus, the principal directions of $\mathbf{\Delta}$ represent normals to potential weak planes, with the weakest plane being normal to the principal direction associated with the largest principal value of $\mathbf{\Delta}$. In this sense, $\mathbf{\Delta}$ acts like a structural tensor to specify the directionality of tensile failure. Moreover, $\mathbf{\Delta}$ is determined by the evolution equation

$$\dot{\mathbf{\Delta}} = \mathbf{W\Delta} + \mathbf{\Delta W}^{\mathrm{T}} + m_\Delta \mathbf{A}_\Delta,$$
$$\mathbf{A}_\Delta = \left[\frac{\langle \Gamma_{\mathrm{f1}}\rangle\beta_1}{(1+\Delta_1)^{n_\Delta}}(\mathbf{p}_1\otimes\mathbf{p}_1) + \frac{\langle \Gamma_{\mathrm{f2}}\rangle\beta_2}{(1+\Delta_2)^{n_\Delta}}(\mathbf{p}_2\otimes\mathbf{p}_2) + \frac{\langle \Gamma_{\mathrm{f3}}\rangle\beta_3}{(1+\Delta_3)^{n_\Delta}}(\mathbf{p}_3\otimes\mathbf{p}_3)\right], \tag{43}$$

where m_Δ and n_Δ are material constants, $\mathbf{W}$ is the skew-symmetric part of the velocity gradient, and $\mathbf{A}_\Delta$ determines the direction of increase in damage. This is one of simplest equations that allows for directional dependence of damage and remains properly invariant under superposed rigid body motions (SRBM).

Specifically, under SRBM the tensors

$$\{\mathbf{B}'_{\mathrm{e}}, \mathbf{A}_{\mathrm{p}}, \mathbf{A}_{\mathrm{v}}, \mathbf{\Delta}, \mathbf{A}_\Delta\}, \tag{44}$$

each obey the transformation relations of the type

$$\mathbf{B}'^{+}_{\mathrm{e}} = \mathbf{Q}\mathbf{B}'_{\mathrm{e}}\mathbf{Q}^{\mathrm{T}}, \tag{45}$$

where a superposed (+) denotes the value of a quantity in the superposed configuration, and $\mathbf{Q}$ is a proper orthogonal function of time only

$$\mathbf{Q} = \mathbf{Q}(t), \qquad \mathbf{Q}^{\mathrm{T}}\mathbf{Q} = \mathbf{I}, \qquad \det(\mathbf{Q}) = 1. \tag{46}$$

Also, the scalars

$$\{J_{\mathrm{e}}, \theta, \phi, \phi_{\mathrm{I}}, \phi_{\mathrm{f}}, \Delta_i\}, \tag{47}$$

remain unaltered by SRBM.

4. Specific constitutive equations

The constitutive equation for the Helmholtz free energy is specified by (Rubin et al., 2000)

$$\rho_{\mathrm{s0}}\psi_{\mathrm{s}} = \rho_{\mathrm{s0}}\widehat{\psi}_{\mathrm{s1}}(J_{\mathrm{e}},\theta) + \tfrac{1}{2}G(J_{\mathrm{e}},\theta)(\alpha_1-3),$$
$$\rho_{\mathrm{s0}}\widehat{\psi}_{\mathrm{s1}} = \rho_{\mathrm{s0}}c_{\mathrm{sv}}[(\theta-\theta_0)-\theta\ln(\theta/\theta_0)] - (\theta-\theta_0)f_1(J_{\mathrm{e}}) + f_2(J_{\mathrm{e}}), \tag{48}$$

where $\widehat{\psi}_{\mathrm{s1}}$ characterizes the main thermomechanical pressure response, c_{sv} is the specific heat at constant volume, θ_0 is the reference temperature, f_1 and f_2 are functions of J_{e} only, and G is the shear modulus. Using this form, the entropy η in (21d), the specific internal energy ε, and the pressure p_{s} in (25c) become

$$\eta = \eta_{\mathrm{s}} = \eta_{\mathrm{s1}} + \eta'_{\mathrm{s}}, \qquad \eta_{\mathrm{s1}} = -\frac{\partial\widehat{\psi}_{\mathrm{s1}}}{\partial\theta} = \rho_{\mathrm{s0}}c_{\mathrm{sv}}\ln(\theta/\theta_0) + f_1, \qquad \rho_{\mathrm{s0}}\eta'_{\mathrm{s}} = -\frac{1}{2}\frac{\partial G}{\partial\theta}(\alpha_1-3),$$
$$\varepsilon = \psi + \theta\eta = \varepsilon_{\mathrm{s1}} + \varepsilon'_{\mathrm{s}}, \qquad \rho_{\mathrm{s0}}\varepsilon_{\mathrm{s1}} = \rho_{\mathrm{s0}}(\psi_{\mathrm{s1}} + \theta\eta_{\mathrm{s1}}) = \rho_{\mathrm{s0}}c_{\mathrm{sv}}(\theta-\theta_0) + \theta_0 f_1 + f_2,$$
$$\rho_{\mathrm{s0}}\varepsilon'_{\mathrm{s}} = \frac{1}{2}\left[G - \theta\frac{\partial G}{\partial\theta}\right](\alpha_1-3),$$
$$p_{\mathrm{s}} = p_{\mathrm{s1}} + p'_{\mathrm{s}}, \qquad p_{\mathrm{s1}}(J_{\mathrm{e}},\theta) = -\rho_{\mathrm{s0}}\frac{\partial\widehat{\psi}_{\mathrm{s1}}}{\partial J_{\mathrm{e}}} = (\theta-\theta_0)\frac{\mathrm{d}f_1}{\mathrm{d}J_{\mathrm{e}}} - \frac{\mathrm{d}f_2}{\mathrm{d}J_{\mathrm{e}}}, \qquad p'_{\mathrm{s}}(J_{\mathrm{e}},\alpha_1,\theta) = -\frac{1}{2}\frac{\partial G}{\partial J_{\mathrm{e}}}(\alpha_1-3). \tag{49}$$

Moreover, the functional forms for f_1 and f_2 can be specified to be consistent with the usual Mie–Gruneisen equation of state for the part p_{s1} of the pressure (Rubin et al., 2000)

$$p_{s1} = p_{sH} + \rho_{s0}\gamma_{s0}[\varepsilon_{s1} - \varepsilon_{sH}], \qquad e_v = 1 - J_e, \qquad p_{sH} = \frac{\rho_{s0}C_{s0}^2 e_v}{(1 - Se_v)^2}, \qquad \varepsilon_{sH} = \frac{C_{s0}^2 e_v^2}{2(1 - Se_v)^2}, \tag{50}$$

where p_{sH} and ε_{sH} are the pressure and internal energy associated with the Hugoniot of the solid material, the Gruneisen gamma γ_{s0} controls the temperature dependence of the pressure, e_v is a measure of elastic volumetric compression, and the shock velocity D has been taken to be a linear function of the particle velocity v of the form

$$D = C_{s0} + Sv, \tag{51}$$

with C_{s0} and S being material constants. For simplicity, the form of the Gruneisen gamma γ_s has been taken so that $\rho_s\gamma_s = \rho_{s0}\gamma_{s0}$ is constant. It then follows from (Rubin et al., 2000) that

$$f_1 = \rho_{s0}c_{sv}\gamma_{s0}\ln(J_e), \tag{52}$$

and f_2 is determined by quadratures. Also, the shear modulus G can be specified by a form similar to that suggested by Steinberg et al. (1980) [see Rubin et al. (2000)]. However, for the examples considered in the next section, G is taken to be constant

$$G = G_0. \tag{53}$$

The evolution equations (36d), (36e) and (43) require specification of the constitutive functions

$$\{\Gamma_p, \Gamma_I, \Gamma_{fi}\}, \tag{54}$$

and the values m_Δ and n_Δ. If the functions (54) are homogeneous functions of order one in deformation rate $\mathbf{D}$ and/or $\dot{\theta}$, then the associated evolution equations predict rate-independent response. Otherwise, they predict rate-dependent response.

Since the main objective of this work is to propose a model for directional tensile failure, the discussion of models for plasticity (associated with Γ_p) and porous compaction and dilation (associated with Γ_I) will remain rather general. However, a specific model will be proposed for directional tensile failure (associated with Γ_{fi}) which can be used with other specific models for Γ_p and Γ_I.

A number of models for rate-independent plasticity have been proposed and a critical review of finite plasticity theory can be found in Naghdi (1990). More specifically, for rate-independent theories with a yield function (e.g. Green and Naghdi, 1965; Naghdi and Trapp, 1975) the value of Γ_p is determined by a consistency conditions which requires the yield function to remain zero during plastic loading. Alternatively, within the context of rate-dependent viscoplasticity, Γ_p can be specified by an overstress-type model (e.g. Malvern, 1951; Perzyna et al., 1963) or by a unified model which combines plasticity and creep into one inelastic deformation rate (e.g. Bodner and Partom, 1972, 1975; Bodner, 1987). In particular, Γ_p is usually taken to be a function of the von-Mises stress σ_e

$$\sigma_e^2 = \tfrac{3}{2}\mathbf{T}' \cdot \mathbf{T}', \tag{55}$$

and hardening variables. For the examples considered later, viscoplasticity is considered using the yield function

$$\Gamma_p = \Gamma_{p0}\left\langle 1 - \frac{Y}{\sigma_e} \right\rangle, \qquad Y = Y(p) = Y_0F_1(p), \qquad F_1(p) = 1 + \frac{k_1\langle p \rangle}{1 + k_2\langle p \rangle}, \tag{56}$$

with Y being the yield strength and $\{\Gamma_{p0}, Y_0, k_1, k_2\}$ being non-negative constants. When Γ_{p0} becomes infinite, the response becomes rate-independent and is the same as that characterized by the yield function

$$\gamma = 1 - \frac{Y}{\sigma_e} \leqslant 0. \tag{57}$$

Also, when k_1 is non-zero then the model includes pressure dependence of the yield strength which is typical of geological materials.

A number of models for porous compaction have been presented in the literature (e.g. Herrmann, 1969; Butkovich, 1973; Rubin et al., 1996). Additional models which include both porous compaction ($\Gamma_I \leqslant 0$) and porous dilation ($\Gamma_I > 0$) have also been presented (Rubin et al., 2000). However, for the example problems considered later, these effects of porous compaction and dilation are ignored, so that

$$\Gamma_I = 0. \tag{58}$$

Returning to the model for directional tensile failure the functions Γ_{fi} are specified in the simple forms

$$\Gamma_{fi} = \Gamma_{fi}(\sigma_i) = \Gamma_{f0}\left[\left\langle \frac{\sigma_i - T_{fi}}{T_f} \right\rangle - \frac{\phi_f}{a_f + \phi_f}\left\langle \frac{-(\sigma_i + T_{fi})}{T_f} \right\rangle (\Delta_i)^{n_f}\right] \quad \text{(no sum on } i\text{)}, \tag{59}$$

where Γ_{f0}, T_f, a_f and n_f are non-negative material constants. Also, the values of T_{fi} are given by

$$T_{fi} = \langle 1 - \Delta_i \rangle T_f. \tag{60}$$

It then follows that (59) predicts dilation for σ_i greater than the tensile failure value T_{fi} and it predicts compaction for σ_i less than the compressive failure $(-T_{fi})$. Since T_{fi} is non-negative, these functions automatically satisfy the restrictions (37). The term $\phi_f/(a_f + \phi_f)$ eliminates further compaction when the failure porosity vanishes and the term $(\Delta_i)^{n_f}$ reduces compaction due to tensile failure in directions that have not been sufficiently damaged.

5. Numerical integration procedures

The constitutive equations (48)–(53) characterize the thermoelastic response in terms of algebraic equations that depend on the material constants

$$\{\rho_{s0}, C_{s0}, S, \gamma_{s0}, \theta_0, G_0\}, \tag{61}$$

and the evolution equations: (24b) for J; (36d) for ϕ, (36e) for $\mathbf{B}'_e$; (39a) for ϕ_I; and (43) for $\boldsymbol{\Delta}$, depend on the function Γ_I and on the material constants

$$\{Y_0, \Gamma_{p0}\}, \qquad \{m_\Delta, n_\Delta, \Gamma_{f0}, a_f, T_f\}. \tag{62}$$

All of these evolution equations except for (24b) are rate-dependent.

The numerical procedure used to integrate these evolution equations starts with the initial values (at $t = t_1$)

$$\{J(t_1), \mathbf{B}'_e(t_1), \phi_I(t_1), \phi_f(t_1), p(t_1), \sigma_e(t_1), \theta(t_1)\}, \tag{63}$$

assumes that the deformation rate $\mathbf{L}$ is constant during the time step $[t_1 \leqslant t \leqslant t_2; \Delta t = t_2 - t_1]$ and suggests the following five step procedure:

Step 1: Calculate the final values $\{J(t_2), \varepsilon(t_2)\}$ using the balance of energy based on the previous stresses and the current rate of deformation.

Step 2: Calculate the trial values $\{\mathbf{B}'^*_e, p^*, \sigma^*_e\}$ assuming an elastic step with no effect of viscoplasticity ($\Gamma_p = 0$), isotropic porosity ($\Gamma_I = 0$) or tensile failure ($\Gamma_{fi} = 0$), and with no change in temperature.

Step 3: Calculate the final value $\{\phi_{\rm I}(t_2)\}$ and the new trial values $\{\mathbf{B}'^{**}_{\rm e}, p^{**}, \sigma^{**}_{\rm e}\}$ correcting for the effects of plasticity and isotropic porosity, but neglecting tensile failure ($\Gamma_{{\rm f}i} = 0$) and neglecting change in temperature.

Step 4: Calculate the final values

$$\{\mathbf{\Delta}(t_2), \mathbf{B}'_{\rm e}(t_2), \phi_{\rm f}(t_2)\}, \tag{64}$$

correcting for the effect of tensile failure and neglecting change in temperature.

Step 5: Calculate the final value of temperature using $\varepsilon(t_2)$ and requiring consistency with the constitutive equation for ε at the end of the time step with updated values of all other quantities.

The order of these steps is specified partly by the rate of each of the physical processes, with the fastest process being performed first, and partly by the structure of the computer code used to calculate the material response. Some applications may suggest a different order of the steps in the numerical scheme.

Specifically, the velocity gradient $\mathbf{L}$ is assumed to be constant during the time step and Step 1 integrates Eq. (24b) to obtain

$$J(t_2) = J(t_1)\left[\frac{1 + \Delta t\langle \mathbf{D}\cdot\mathbf{I}\rangle}{1 + \Delta t\langle -\mathbf{D}\cdot\mathbf{I}\rangle}\right]. \tag{65}$$

Then, assuming adiabatic conditions ($r = 0, \mathbf{q} = 0$), the energy equation (5a) is integrated using the previous values of the stress $\mathbf{T}(t_1)$ and the constant value of $\mathbf{D}$, so that

$$\varepsilon(t_2) = \varepsilon(t_1) + \Delta t\mathbf{T}(t_1)\cdot\mathbf{D}. \tag{66}$$

Step 2 integrates Eq. (36e) to obtain the trial elastic distortion $\mathbf{B}'^{*}_{\rm e}$

$$\mathbf{B}'^{*}_{\rm e} = \mathbf{B}'_{\rm e}(t_1) + \Delta t\left[\mathbf{L}\mathbf{B}'_{\rm e} + \mathbf{B}'_{\rm e}\mathbf{L}^{\rm T} - \tfrac{2}{3}(\mathbf{D}\cdot\mathbf{I})\mathbf{B}'_{\rm e}\right]. \tag{67}$$

Using the values $\{J(t_2), \mathbf{B}'^{*}_{\rm e}, \theta(t_1), \phi(t_1), \phi_{\rm I}(t_1)\}$, the quantities $\{p^*, \sigma^*_{\rm e}, Y^* = Y(p^*)\}$ are determined. Depending on the functional form for $\Gamma_{\rm I}$ in (39a) it may be necessary to iteratively solve this evolution equation to determine the final value $\phi_{\rm I}(t_2)$. However, this procedure is not described in detail because a specific functional form for $\Gamma_{\rm I}$ is not specified.

The effects of viscoplasticity are determined by the procedures described in Rubin (1989) and Rubin and Attia (1996). Specifically, the effects of plasticity can be determined using a radial return algorithm which requires implicit integration of the evolution equation, such that

$$\begin{gathered}(1-\lambda) = \Delta t\Gamma_{\rm p}\lambda, \qquad \sigma^{**}_{\rm e} = \lambda\sigma^*_{\rm e}, \qquad \mathbf{B}''^{**}_{\rm e} = \lambda\mathbf{B}''^{*}_{\rm e}, \qquad \mathbf{B}''^{*}_{\rm e} = \mathbf{B}'^{*}_{\rm e} - \tfrac{1}{3}(\mathbf{B}'^{*}_{\rm e}\cdot\mathbf{I})\mathbf{I}, \\ \mathbf{B}''^{**}_{\rm e} = \mathbf{B}'^{**}_{\rm e} - \tfrac{1}{3}(\mathbf{B}'^{**}_{\rm e}\cdot\mathbf{I})\mathbf{I},\end{gathered} \tag{68}$$

where λ is the scale factor used to reduce the trial stress. Now, with the help of (56) it follows that

$$\lambda = 1 \quad \text{for } \sigma^*_{\rm e} \leqslant Y^*, \qquad \lambda = \frac{1 + \frac{\Delta t\Gamma_{\rm p0}Y^*}{\sigma^*_{\rm e}}}{1 + \Delta t\Gamma_{\rm p0}} \quad \text{for } \sigma^*_{\rm e} > Y^*. \tag{69}$$

Next, the procedure moves to Step 4 where the effects of tensile failure are considered. To this end, the evolution equations (36e) and (39b) are evaluated implicitly and are written in the forms

$$\mathbf{B}'_{\rm e}(t_2) = \mathbf{B}'^{**}_{\rm e} - 2\beta_1(t_2)\Delta t\Gamma'_{\rm f1}(\mathbf{p}_1\otimes\mathbf{p}_1) - 2\beta_2(t_2)\Delta t\Gamma'_{\rm f2}(\mathbf{p}_2\otimes\mathbf{p}_2) - 2\beta_3(t_2)\Delta t\Gamma'_{\rm f3}(\mathbf{p}_3\otimes\mathbf{p}_3), \tag{70a}$$

$$\Delta\phi_{\rm f} = \phi_{\rm f}(t_2) - \phi_{\rm f}(t_1) = [1 - \phi_{\rm I}(t_2) - \phi_{\rm f}(t_2)]\Delta t\Gamma_{\rm f}, \tag{70b}$$

where $\mathbf{p}_i$ are the eigenvectors of $\mathbf{B}'^{**}_{\rm e}$ and β^{**}_i are its eigenvalues so that $\mathbf{B}'^{**}_{\rm e}$ can be expressed in the spectral form

$$\mathbf{B}_e'^{**} = \beta_1^{**}(\mathbf{p}_1 \otimes \mathbf{p}_1) + \beta_2^{**}(\mathbf{p}_2 \otimes \mathbf{p}_2) + \beta_3^{**}(\mathbf{p}_3 \otimes \mathbf{p}_3). \tag{71}$$

Thus, Eq. (70a) can be rewritten as three scalar equations

$$\Delta\beta_i = \beta_i(t_2) - \beta_i^{**} = -2\beta_i(t_2)\Delta t \Gamma'_{fi} \quad \text{(no sum on } i\text{)}, \tag{72}$$

where only two of these equations are independent since $\mathbf{B}'_e$ is a unimodular tensor. Furthermore, using the constitutive equations (25), (29), (48)–(50), it follows that p and σ'_i become

$$p = (1-\phi)\left[p_{sH} + \rho_{s0}\gamma_{s0}(\varepsilon_{s1} - \varepsilon_{sH}) + p'_s\right], \qquad \sigma'_i = (1-\Phi)J^{-1}G\left[\beta_i - \tfrac{1}{3}(\mathbf{B}'_e \cdot \mathbf{I})\right]. \tag{73}$$

Thus, assuming the stresses remain relatively small whenever tensile failure is active (J_e and β_i are each close to unity), the final values of p and σ'_i are approximated by

$$p(t_2) \approx p^{**} + \rho_{s0}C_{s0}^2\Delta\phi_f, \qquad \sigma'_i(t_2) = \sigma_i'^{**} + (1-\Phi)J(t_2)^{-1}G_0\left[\Delta\beta_i - \tfrac{1}{3}(\Delta\beta_1 + \Delta\beta_2 + \Delta\beta_3)\right]. \tag{74}$$

Moreover, Eqs. (70b) and (72) are further approximated by replacing $\phi_f(t_2)$ with $\phi_f(t_1)$, and $\beta_i(t_2)$ with unity, on the right-hand sides of these equations to obtain

$$\Delta\phi_f = [1 - \phi_I(t_2) - \phi_f(t_1)]\Delta t\Gamma_f, \qquad \Delta\beta_i = -2\Delta t\Gamma'_{fi}. \tag{75}$$

Thus, the principal stresses can be approximated by

$$\sigma_i(t_2) = \sigma_i^{**} - \left[\{1 - \phi_I(t_2) - \phi_f(t_1)\}\rho_{s0}C_{s0}^2\right]\Delta t\Gamma_f - \left[2(1-\Phi)J(t_2)^{-1}G_0\right]\Delta t\Gamma'_{fi}, \tag{76}$$

which can be rewritten in the form

$$\begin{aligned}
&\sigma_i(t_2) = \sigma_i^{**} - C_{ij}\Gamma_{fj},\\
&C_{11} = C_{22} = C_{33} = \left[\{1 - \phi_I(t_2) - \phi_f(t_1)\}\rho_{s0}C_{s0}^2 + \tfrac{4}{3}(1-\Phi)J(t_2)^{-1}G_0\right]\Delta t > 0,\\
&C_{12} = C_{13} = C_{23} = \left[\{1 - \phi_I(t_2) - \phi_f(t_1)\}\rho_{s0}C_{s0}^2 - \tfrac{2}{3}(1-\Phi)J(t_2)^{-1}G_0\right]\Delta t > 0,\\
&C_{ij} = C_{ji}.
\end{aligned} \tag{77}$$

Next, the estimates $\mathbf{\Delta}^*$ and Δ_i^* of $\mathbf{\Delta}$ and Δ_i, respectively, are obtained by Euler integration of the rotational part of (43)

$$\mathbf{\Delta}^* = \mathbf{\Delta}(t_1) + \Delta t[\mathbf{W}\mathbf{\Delta}(t_1) + \mathbf{\Delta}(t_1)\mathbf{W}^T], \qquad \Delta_i^* = \langle \mathbf{\Delta}^* \cdot (\mathbf{p}_i \otimes \mathbf{p}_i)\rangle \quad \text{(no sum on } i\text{)}. \tag{78}$$

Then, the values of Γ_{fi} in (77) are determined by evaluating the constitutive equations (59), with the help of the final values $\sigma_i(t_2)$ and the estimates Δ_i^*, such that (59) can be rewritten in the forms

$$\Gamma_{fi} = \Gamma_{f0}\left[\left\langle \frac{\sigma_i(t_2) - T_{fi}(t_1)}{T_f}\right\rangle - \frac{\phi_f(t_1)}{a_f + \phi_f(t_1)}\left\langle \frac{-\{\sigma_i(t_2) + T_{fi}(t_1)\}}{T_f}\right\rangle (\Delta_i^*)^{n_f}\right] \quad \text{(no sum on } i\text{)}. \tag{79}$$

Substituting (79) into (77) yields an equation which can be written in the matrix form

$$A_{ij}\sigma_j(t_2) = B_i. \tag{80}$$

Specifically, since each of Γ_{fi} can be negative, zero, or positive, there are 27 combinations of the matrix A_{ij} and the vector B_i. To record these values it is convenient to introduce the auxiliary variables I_i by the equations

$$I_i = -1 \quad \text{for } \Gamma_{fi} < 0, \qquad I_i = 0 \quad \text{for } \Gamma_{fi} = 0, \qquad I_i = 1 \quad \text{for } \Gamma_{fi} > 0, \tag{81}$$

so that

$$A_{ij} = \delta_{ij} + \langle -I_j \rangle C_{ij} \frac{\Gamma_{\mathrm{f0}}}{T_{\mathrm{f}}} \frac{\phi_{\mathrm{f}}}{a_{\mathrm{f}} + \phi_{\mathrm{f}}} (\Delta_j^*)^{n_{\mathrm{f}}} + \langle I_j \rangle C_{ij} \frac{\Gamma_{\mathrm{f0}}}{T_{\mathrm{f}}} \quad \text{(no sum on } j\text{)},$$
$$B_i = \sigma_i^{**} + \sum_{j=1}^{3} \left[-\langle -I_j \rangle C_{ij} \frac{\Gamma_{\mathrm{f0}}}{T_{\mathrm{f}}} \frac{\phi_{\mathrm{f}}}{a_{\mathrm{f}} + \phi_{\mathrm{f}}} (\Delta_j^*)^{n_{\mathrm{f}}} T_{\mathrm{f}j} + \langle I_j \rangle C_{ij} \frac{\Gamma_{\mathrm{f0}}}{T_{\mathrm{f}}} T_{\mathrm{f}j} \right], \tag{82}$$

where δ_{ij} is the Kronecker delta symbol. The solution of (80) is obtained by guessing a branch of the solution (based on the values of $\Gamma_{\mathrm{f}i}$ associated with estimates of the stresses σ_i), then using the appropriate values of A_{ij} and B_i and solving (80) for the updated σ_i. The solution is considered to be correct if the updated values of $\Gamma_{\mathrm{f}i}$ correspond to the same branch that is being checked.

At present it is not known how to analytically analyze this solution procedure to determine if the solution is unique and, if so, to determine the optimal path to the solution. Consequently, the solution procedure was tested numerically by specifying values of σ_i^{**} as random positions in a cube $[-10T_{\mathrm{f}} \leqslant \sigma_i^{**} \leqslant 10T_{\mathrm{f}}]$. The results of these calculations with one million random values indicate that about 70% of the guesses based on σ_i^{**} yielded the correct solution branch. The correct solution was obtained by the second guess in about 10–20% of the trials. Occasionally, either a few multiple solutions are found, or an infinite loop occurred with the solution bouncing between a few trial solutions because of floating point inaccuracies. However, for each of these cases the multiple solutions or the trial solutions were close to each other (and were often near the boundaries of expansion and contraction). Consequently, it was decided to terminate the solution search either when a solution is found or after a maximum of seven iterations (which exceeds the typical number of iterations required in the random calculations).

Once the solution of (80) is obtained, the updated values of $\Gamma_{\mathrm{f}i}$ are used in (35) to determine Γ_{f} and $\Gamma'_{\mathrm{f}i}$. Specifically, the solutions of (72) and (74) are modified to obtain

$$\overline{\beta}_i = \beta_i^{**} \left[\frac{1 + 2\Delta t \langle -\Gamma'_{\mathrm{f}i} \rangle}{1 + 2\Delta t \langle \Gamma'_{\mathrm{f}i} \rangle} \right], \qquad \beta_i(t_2) = \left[\overline{\beta}_1 \overline{\beta}_2 \overline{\beta}_3 \right]^{-1/3} \overline{\beta}_i, \quad \text{(no sum on } i\text{)},$$
$$\mathbf{B}'_{\mathrm{e}}(t_2) = \beta_1(t_2)\mathbf{p}_1 \otimes \mathbf{p}_1 + \beta_2(t_2)\mathbf{p}_2 \otimes \mathbf{p}_2 + \beta_3(t_2)\mathbf{p}_3 \otimes \mathbf{p}_3, \tag{83}$$
$$\phi_{\mathrm{f}}(t_2) = \left\langle 1 - \phi_{\mathrm{I}}(t_2) - \{1 - \phi_{\mathrm{f}}(t_1) - \phi_{\mathrm{I}}(t_2)\} \left[\frac{1 + \Delta t \langle -\Gamma_{\mathrm{f}} \rangle}{1 + \Delta t \langle \Gamma_{\mathrm{f}} \rangle} \right] \right\rangle,$$

which ensure that $\beta_i(t_2)$ remain positive, $\mathbf{B}'_{\mathrm{e}}(t_2)$ remains a unimodular tensor, $\phi_{\mathrm{f}}(t_2)$ is non-negative and $\phi(t_2)$ is smaller than unity. Furthermore, the final value $\mathbf{\Delta}(t_2)$ of the damage tensor is obtained by using the updated values of β_i and $\Gamma_{\mathrm{f}i}$ in the formula

$$\mathbf{\Delta}(t_2) = \mathbf{\Delta}^* + \Delta t m_{\Delta} \left[\frac{\langle \Gamma_{\mathrm{f1}} \rangle \beta_1(t_2)}{(1 + \Delta_1^*)^2} (\mathbf{p}_1 \otimes \mathbf{p}_1) + \frac{\langle \Gamma_{\mathrm{f2}} \rangle \beta_2(t_2)}{(1 + \Delta_2^*)^2} (\mathbf{p}_2 \otimes \mathbf{p}_2) + \frac{\langle \Gamma_{\mathrm{f3}} \rangle \beta_3(t_2)}{(1 + \Delta_3^*)^2} (\mathbf{p}_3 \otimes \mathbf{p}_3) \right]. \tag{84}$$

From (49) the constitutive equation for the internal energy ε takes the general form

$$\varepsilon = \widehat{\varepsilon}(J, \theta, \phi, \alpha_1). \tag{85}$$

Thus, the final temperature $\theta(t_2)$ associated with Step 5 is determined by using the value $\varepsilon(t_2)$ obtained in (66) and solving the equation

$$\widehat{\varepsilon}(J(t_2), \theta(t_2), \phi(t_2), \alpha_1(t_2)) = \varepsilon(t_2). \tag{86}$$

When G is a function of temperature, this equation is a non-linear function of $\theta(t_2)$ which must be solved iteratively. However, for constant G (53), the constitutive equation (49) for ε is a linear function of θ, which can be solved to obtain

$$\theta(t_2) = \theta_0 + \frac{1}{\rho_{s0} c_{sv}} \left[\rho_{s0} \varepsilon(t_2) - \theta_0 f_1(J_e) - f_2(J_e) + \frac{1}{2} G_0(\alpha_1 - 3) \right], \tag{87}$$

with J_e and α_1 being the updated values associated with $t = t_2$.

6. Examples

The objective of the example problems considered in this section is to demonstrate typical features of the proposed model and not to match any particular set of data for a specific material. Specifically, in order to examine the response of this model it is convenient to consider the response to homogeneous deformation which is characterized by specifying a loading history for the velocity gradient $\mathbf{L}$. Moreover, the deformation gradient $\mathbf{F}$ is determined by integrating the evolution equation

$$\dot{\mathbf{F}} = \mathbf{L}\mathbf{F}, \tag{88}$$

and the Lagrangian strain $\mathbf{E}$ is defined by

$$\mathbf{E} = \tfrac{1}{2}(\mathbf{F}^T\mathbf{F} - \mathbf{I}). \tag{89}$$

For the examples considered below, the evolution equations (15b), (24b), (39a,b), (40a), (43) and (88), are integrated subject to the initial conditions

$$J = 1, \qquad \mathbf{B}'_e = \mathbf{I}, \qquad \phi_I = 0, \qquad \phi_f = 0, \qquad \mathbf{\Delta} = 0, \qquad \mathbf{F} = \mathbf{I}, \qquad \varepsilon_p = 0. \tag{90}$$

Thus, since $\Gamma_I = 0$, the porosity $\phi_I = 0$ and the total porosity $\phi = \phi_f$. Furthermore, let $\{L_{ij}, E_{ij}, T_{ij}, \Delta_{ij}\}$ be the components of the tensors $\{\mathbf{L}, \mathbf{E}, \mathbf{T}, \mathbf{\Delta}\}$, respectively, relative to the fixed rectangular Cartesian base vectors $\mathbf{e}_i$.

The loading history is specified by a combination of the following deformation paths:

Uniaxial strain in the $\mathbf{e}_1$ direction

$$\mathbf{L} = D\mathbf{e}_1 \otimes \mathbf{e}_1, \tag{91}$$

Uniaxial strain in the $\mathbf{e}_2$ direction

$$\mathbf{L} = D\mathbf{e}_2 \otimes \mathbf{e}_2, \tag{92}$$

Isochoric deformation in the $\mathbf{e}_1$–$\mathbf{e}_2$ plane

$$\mathbf{L} = \frac{D}{\sqrt{2}}[\mathbf{e}_1 \otimes \mathbf{e}_1 - \mathbf{e}_2 \otimes \mathbf{e}_2], \tag{93}$$

Isochoric simple shear in the $\mathbf{e}_1$–$\mathbf{e}_2$ plane

$$\mathbf{L} = \sqrt{2}D\mathbf{e}_1 \otimes \mathbf{e}_2, \tag{94}$$

Pure dilation

$$\mathbf{L} = \frac{D}{\sqrt{3}}\mathbf{I}, \tag{95}$$

where the rates of deformation have been normalized to have the same magnitude of the deformation rate $\mathbf{D}$. Unless otherwise stated, the value of D is specified by

$$D = \pm 10 \text{ s}^{-1}, \tag{96}$$

which is characteristic of mild shock loading in large rock structures.

Typical material properties of hard granite are obtained from Handin (1966), and Schock et al. (1973) and specified in Tables 1–3 and are used in the following examples. For simplicity, the Gruneissen gamma γ_{s0} is specified to be zero and no values are specified for c_{sv} and θ_0, since temperature is not needed for the calculations. Also, the value of Γ_{p0} is taken to be infinity in order to obtain rate-independent plastic response.

For these material parameters, tensile failure can occur for low pressures (i.e. near free surfaces) but not for higher pressures. Due to the complicated loading histories being presented it is convenient to exhibit all quantities as functions of time. For each of the loading histories, figures (a) show the strains, figures (b) show the stresses, figures (c) show the porosity and plastic strains, and figures (d) show maximum principal value Δ_{max} and minimum of principal value Δ_{min} of $\mathbf{\Delta}$ in the $\mathbf{e}_1$–$\mathbf{e}_2$ plane as well as its component Δ_{33}. For some of the loadings figures (e) show the angle δ characterizing the principal direction $\mathbf{p}_{max}$ associated with Δ_{max}

$$\mathbf{p}_{max} = \cos\delta\mathbf{e}_1 + \sin\delta\mathbf{e}_2. \tag{97}$$

Fig. 1 shows the response to a cycle of uniaxial extension and contraction in the $\mathbf{e}_1$ direction, followed by a cycle of uniaxial extension and contraction in the $\mathbf{e}_2$ direction. For this loading the angle δ equals zero so it is not plotted. During the first extension in the $\mathbf{e}_1$ direction, tensile failure occurs in T_{11} and the values of T_{22}

Table 1
Typical material properties for the thermoelastic response of granite

	Value	Equation
Φ	0	(23a)
ρ_{s0} (Mg/m^3)	2.67	(23a)
C_{s0} (km/s)	4.20	(50)
S	1.50	(50)
γ_{s0}	0.0	(50)
c_{sv} (J/Kg/K)	–	(48)
θ_0 (K)	–	(48)
G_0 (GPa)	28.80	(53)

Table 2
Typical material properties for the plastic response of granite

	Value	Equation
Γ_{p0} (s^{-1})	∞	(56)
Y_0 (GPa)	0.10	(56)
k_1 (GPa^{-1})	17.0	(56)
k_2 (GPa^{-1})	0.33	(56)

Table 3
Material properties for tensile failure

	Value	Equation
Γ_{f0} (s^{-1})	10^3	(59)
a_f	10^{-6}	(59)
T_f (MPa)	10.0	(59)
n_f	3.0	(59)
m_Δ (s^{-1})	10^3	(43)
n_Δ	2.0	(43)

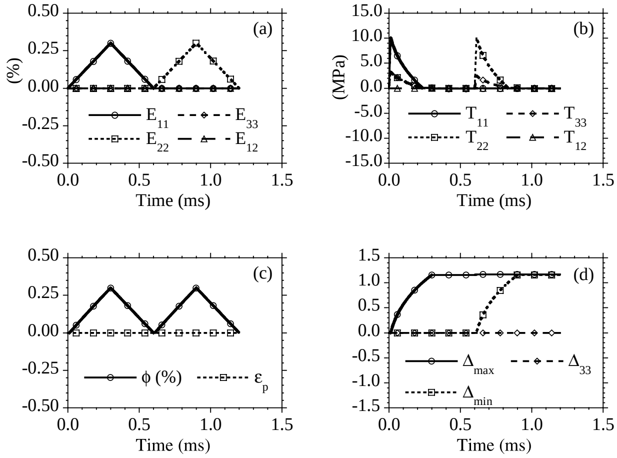

Fig. 1. Response to cycles of uniaxial strain.

and T_{33} are equal. Porosity opens during extension and closes during contraction (with almost zero stress once damage is complete). During the first extension in the $\mathbf{e}_2$ direction tensile failure occurs in T_{22} at the virgin tensile strength since this direction was not damaged during the first part of the cycle of loading (see Fig. 1d). Also, since the $\mathbf{e}_1$ direction has already been damaged, the value of T_{11} remains near zero during

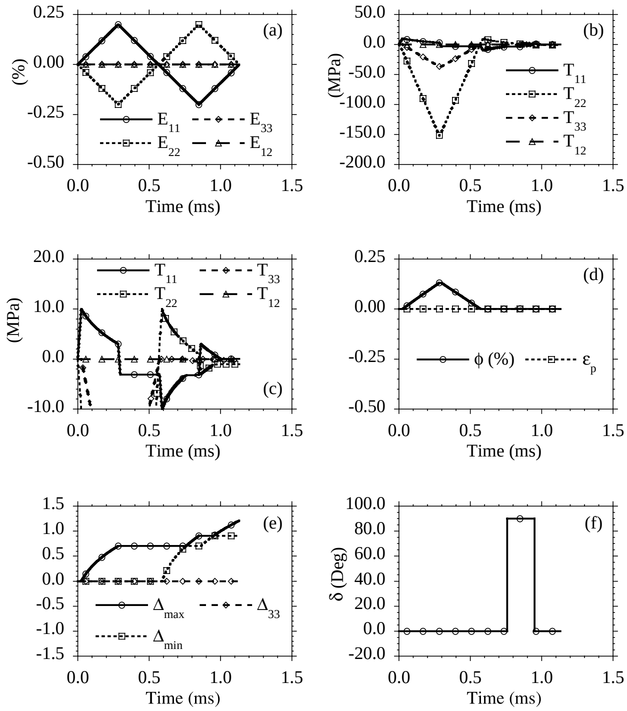

Fig. 2. Response to cycles of isochoric deformation.

this extension, whereas the value of T_{33} becomes tensile. As T_{22} fails, porosity again opens during extension and closes during contraction (with almost zero stress once damage is complete).

Fig. 2 shows the response to a cycle of isochoric deformation with simultaneous deformation occurring in both the $\mathbf{e}_1$ and $\mathbf{e}_2$ directions. Specifically, the first part of the loading is a cycle with extension ($E_{11} \geqslant 0$) in $\mathbf{e}_1$ direction and contraction ($E_{22} \leqslant 0$) in the $\mathbf{e}_2$ direction, and the second part of the loading, is a cycle of with contraction ($E_{11} \leqslant 0$) in the $\mathbf{e}_1$ direction and extension ($E_{22} \geqslant 0$) in the $\mathbf{e}_2$ direction. Fig. 2c shows an expanded view of the tensile portion of the response shown in Fig. 2b. The main response of directional failure is again captured with tensile failure occurring in the $\mathbf{e}_1$ direction during the first part of the loading and tensile failure occurring in the $\mathbf{e}_2$ direction during the second part of the loading. The main differences between the first and second parts of the loading can be seen in Fig. 2b and d where it is observed that during the first part of the loading there is no damage associated with the $\mathbf{e}_2$ direction so that substantial compression can occur ($T_{22} < 0$ in Fig. 2b) in that direction. This is accompanied with porosity change (Fig. 2d) required to limit the tensile stress T_{11}. In contrast, during the second part of the loading, the $\mathbf{e}_1$ direction has been pre-damaged (Fig. 2e) so the constitutive equations (30), (58)–(60) allow inelastic compression in this direction whenever ϕ_f is non-zero. Moreover, during this part of the loading inelastic extension occurs in the $\mathbf{e}_1$ direction. The net effect is to maintain the porosity near zero. In other words, when the material has been fully damaged in both the $\mathbf{e}_1$ and $\mathbf{e}_2$ directions, the material flows with small deviatoric stresses. This is similar to what would be expected in a granular material with no external pressure.

Fig. 3 shows the response to large deformation simple shear. It can be seen from Fig. 3e that damage initiates in the $\delta = 45°$ direction and porosity grows (Fig. 3c). This causes the pressure to increase so the stress field shown in Fig. 3b is nearly equivalent to uniaxial compression in the direction $\delta = 135°$. It can be seen from Fig. 3c that tensile failure and plastic flow occur simultaneously during this process. Fig. 3e

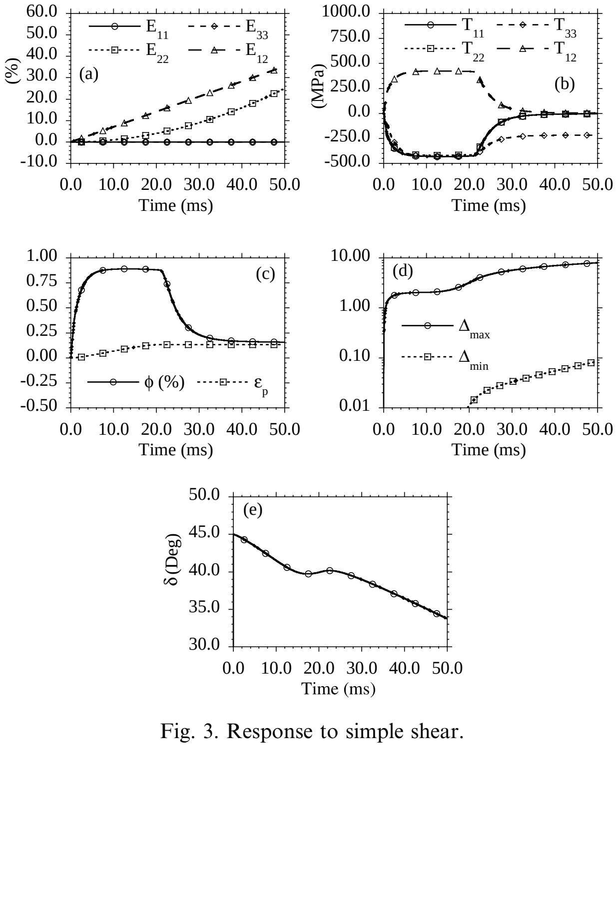

Fig. 3. Response to simple shear.

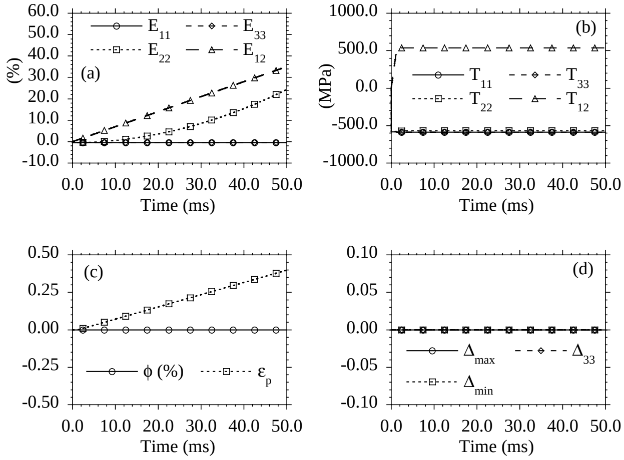

Fig. 4. Response to pure dilation (compression) followed by simple shear.

shows that the damage tensor rotates with δ decreasing. Eventually enough damage accumulates that $\Delta_{\min}$ increases (Fig. 3d) and causes compressive void strain in the $\mathbf{p}_2$ direction with porosity recompression (Fig. 3c) and decrease in pressure (Fig. 3b). After this point the material continues to flow with near zero stresses in the $\mathbf{e}_1$–$\mathbf{e}_2$ plane and compressive T_{33} stress (Fig. 3b). Furthermore, it is noted that Δ_{33} remains zero for this deformation and the values of $\Delta_{\min}$ is small enough that the damage is plotted using a log scale in Fig. 3d.

Fig. 4 shows the response to a small pure dilation (compression) followed by large deformation simple shear. For this problem the pressure is high enough that the material flows plastically with no tensile failure. This response would be typical deep enough under ground where the confining stress in the rock is high.

7. Conclusions

A general theoretical structure has been developed to model directional tensile failure with void opening and closing. The resulting theory is hyperelastic in the sense that the stress is determined by derivatives of the Helmholtz free energy, and the theory is thermodynamically consistent and properly invariant under superposed rigid body motions. Specific constitutive equations for tensile failure have been proposed which satisfy the second law of thermodynamics and can augment rather general constitutive equations for porous compaction and dilation, as characterized by the evolution equation (39a). Moreover, although the model developed here has focused on the phenomena (P3) associated with the inelastic effects of the rate of void opening and closing due to tensile failure, it is possible to include the phenomena (P2) by using a scalar measure of damage to degrade the shear modulus. However, degradation of the non-linear thermomechanical response to dilatation is more difficult.

A numerical algorithm has been developed and the example problems considered in Section 6 show that the model predicts reasonable results to a variety of loading histories. The damage tensor $\mathbf{\Delta}$ that is introduced in this model can be advected using standard methods in Arbitrary Lagrangian Eulerian (ALE) computer codes. Moreover, this constitutive model has been implemented into a general Adaptive Mesh Refinement (AMR) computer code GEODYN developed at Lawrence Livermore Laboratory and simulations of complicated shock loading problems are currently being studied.

Acknowledgements

This research was performed under the auspices of the US Department of Energy by Lawrence Livermore National Laboratory under contract no. W-7405-Eng-48. M.B. Rubin was partially supported by the Fund for Promotion of Research at Technion. Also, the authors would like to acknowledge helpful discussions with L. Glenn, T. Antoun, and W. Moss.

References

Bar-on, E., Rubin, M.B., Yankelevsky, D.Z., 2003. Thermo-mechanical constitutive equations for the dynamic response of Ceramics. Int. J. Solids Struct. in press.

Betten, J., 1985. The classical plastic potential theory in comparison with the tensor function theory. Engng. Fract. Mech. 21, 641–652.

Bodner, S.R., Partom, Y., 1972. A large deformation elastic–viscoplastic analysis of a thick-walled spherical shell. ASME J. Appl. Mech. 39, 751–757.

Bodner, S.R., Partom, Y., 1975. Constitutive equations for elastic–viscoplastic strain-hardening materials. ASME J. Appl. Mech. 42, 385–389.

Bodner, S.R., 1987. Review of unified elastic–viscoplastic theory. In: Miller, A.K. (Ed.), Unified Constitutive Equations for Creep and Plasticity. Elsevier Applied Science Publishers, Barking, England, pp. 273–301.

Butkovich, T.R., 1973. A technique for generating pressure–volume relationships and failure envelopes for rocks. UCRL-51441, Livermore National Laboratory, Livermore, California.

Carol, I., Rizzi, E., Willam, K., 2001. On the formulation of anisotropic elastic degradation. I. Theory based on a pseudo-logarithmic damage tensor rate. Int. J. Solids Struct. 38, 491–518.

Carroll, M., Holt, A.C., 1972. Suggested modification of the p-α model for porous materials. J. Appl. Phys. 43, 759–761.

Curran, D.R., Seaman, L., Shockey, D.A., 1987. Dynamic failure of solids. Physics Reports (A Review Section of Physics Letters) 147, 253–388.

Eckart, C., 1948. The thermodynamics of irreversible processes. iv. The theory of elasticity and anelasticity. Phys. Rev. 73, 373–382.

Elata, D., Rubin, M.B., 1994. Isotropy of strain energy functions which depend only on a finite number of directional strain measures. ASME J. Appl. Mech. 61, 284–289.

Flory, P.J., 1961. Thermodynamic relations for high elastic materials. Trans. Faraday Soc. 57, 829–838.

Green, A.E., Naghdi, P.M., 1965. A general theory of an elastic–plastic continuum. Archiv. Rational Mech. Anal. 18, 251–281.

Green, A.E., Naghdi, P.M., 1977. On thermodynamics and the nature of the second law. Proc. R. Soc. Lond. A 357, 253–270.

Green, A.E., Naghdi, P.M., 1978. The second law of thermodynamics and cyclic processes. ASME J. Appl. Mech. 45, 487–492.

Gurson, A.L., 1977. Continuum theory of ductile rupture by void nucleation and growth: Part 1–yield criteria and flow rules for porous ductile media. ASME J. Engng. Mater. Technol. 99, 2–15.

Handin, J., 1966. Strength and ductility. In: Clark Jr., S.P. (Ed.), Handbook of Physical Constants. Geological Society of America, New York, pp. 223–300.

Herrmann, W., 1969. Constitutive equation for the dynamic compaction of ductile porous materials. J. Appl. Phys. 40, 2490–2499.

Kachanov, L., 1958. On the time to rupture under creep conditions. Izv. Acad. Nauk SSSR, OTN 8, 26–31.

Kachanov, M., Tsurkov, I., Shafiro, B., 1994. Effective moduli of solids with cavities of various shapes. Appl. Mech. Rev. 47, S151–S174.

Krajcinovic, D., 1996. Damage Mechanics. In: North-Holland Series in Applied Mathematics and Mechanics, 51. Elsevier, Amsterdam, The Netherlands.

Leonov, A.I., 1976. Nonequilibrium thermodynamics and rheology of viscoelastic polymer media. Rheologica Acta 15, 85–98.

Malvern, L.E., 1951. The propagation of longitudinal waves of plastic deformation in a bar of material exhibiting a strain-rate effect. ASME J. Appl. Mech. 18, 203–208.

Menzel, A., Steinmann, P., 2001. A theoretical and computational framework for anisotropic continuum damage mechanics at large strains. Int. J. Solids Struct. 38, 9505–9523.

Naghdi, P.M., Trapp, J.A., 1975. The significance of formulating plasticity theory with reference to loading surfaces in strain space. Int. J. Engng. Sci. 13, 785–797.

Naghdi, P.M., 1990. A critical review of the state of finite plasticity. J. Appl. Math. Phys. (ZAMP) 41, 315–394.

Nemat-Nasser, S., Hori, M., 1993. Micromechanics: overall properties of heterogeneous materials. In: Achenbach, J.D., Budiansky, B., Lauwerier, H.A., Saffman, P.G., Van Wijngaarden, J.R. (Eds.), North-Holland Series in Applied Mathematics and Mechanics, vol. 37.

Perzyna, P., 1963. The constitutive equations for rate sensitive plastic materials. Quarterly Appl. Math. 20, 321–332.

Rajendran, A.M., Dietenberger, A.M., Grove, D.J., 1989. A Void-Based Failure Model to Describe Spallation. J. Appl. Phys. 65 (4), 1521–1527.

Schock, R.N., Heard, H.C., Stephens, D.R., 1973. Stress–strain behavior of a granodiorite and two graywackes on compression to 20 kilobars. J. Geophys. Res. 78 (26), 5922–5941.

Rubin, M.B., 1986. An elastic–viscoplastic model for large deformation. Int. J. Engng. Sci. 24, 1083–1095.

Rubin, M.B., 1989. A time integration procedure for large plastic deformation in elastic–viscoplastic metals. J. Math. Phys. (ZAMP) 40, 846–871.

Rubin, M.B., 1994. Plasticity theory formulated in terms of physically based microstructural variables—Part I: Theory. Int. J. Solids Struct. 31, 2615–2634.

Rubin, M.B., 1996. On the treatment of elastic deformation in finite elastic–viscoplastic theory. Int. J. Plasticity 12, 951–965.

Rubin, M.B., 2001. Physical reasons for abandoning plastic deformation measures in finite plasticity and viscoplasticity theory. Arch. Mech. 53, 519–539.

Rubin, M.B., Attia, A., 1996. Calculation of hyperelastic response of finitely deformed elastic–viscoplastic materials. Int. J. Numer. Meth. Engng. 39, 309–320.

Rubin, M.B., Elata, D., Attia, A.V., 1996. Modeling added compressibility of porosity and the thermomechanical response of wet porous rock with application to Mt. Helen Tuff. Int. J. Solids Struct. 33, 761–793.

Rubin, M.B., Vorobiev, O.Yu., Glenn, L.A., 2000. Mechanical and numerical modeling of a porous elastic–viscoplastic material with tensile failure. Int. J. Solids Struct. 37, 1841–1871.

Steinberg, D.J., Cochran, S.G., Guinan, M.W., 1980. A constitutive model for metals applicable at high-strain rates. J. Appl. Phys. 51, 1498–1504.